



# Importance of indole N–H hydrogen bonding in the organization and dynamics of gramicidin channels



Arunima Chaudhuri<sup>a</sup>, Sourav Haldar<sup>a,1</sup>, Haiyan Sun<sup>b</sup>, Roger E. Koeppe II<sup>b</sup>, Amitabha Chattopadhyay<sup>a,\*</sup>

<sup>a</sup> CSIR-Centre for Cellular and Molecular Biology, Uppal Road, Hyderabad 500 007, India

<sup>b</sup> Department of Chemistry and Biochemistry, University of Arkansas, Fayetteville, AR 72701, USA

## ARTICLE INFO

### Article history:

Received 12 August 2013

Received in revised form 10 October 2013

Accepted 14 October 2013

Available online 19 October 2013

### Keywords:

Gramicidin

Indole hydrogen bonding

1-Methylindole

Ion channel

REES

Membrane penetration depth

## ABSTRACT

The linear ion channel peptide gramicidin represents an excellent model for exploring the principles underlying membrane protein structure and function, especially with respect to tryptophan residues. The tryptophan residues in gramicidin channels are crucial for the structure and function of the channel. In order to test the importance of indole hydrogen bonding for the biophysical properties of gramicidin channels, we monitored the effect of N-methylation of gramicidin tryptophans, using a combination of steady state and time-resolved fluorescence approaches along with circular dichroism spectroscopy. We show here that in the absence of the hydrogen bonding ability of tryptophans, tetramethyltryptophan gramicidin (TM-gramicidin) is unable to maintain the single stranded, head-to-head dimeric channel conformation in membranes. Our results show that TM-gramicidin displays a red-shifted fluorescence emission maximum, lower red edge excitation shift (REES), and higher fluorescence intensity and lifetime, consistent with its nonchannel conformation. This is in agreement with the measured location (average depth) of the 1-methyltryptophans in TM-gramicidin using the parallax method. These results bring out the usefulness of 1-methyltryptophan as a fluorescent tool to examine the hydrogen bonding ability of tryptophans in proteins and peptides. We conclude that changes in the hydrogen bonding ability of tryptophans, along with coupled changes in peptide backbone structure induce the loss of single stranded  $\beta^{6,3}$  helical dimer conformation. These results agree with earlier results from size-exclusion chromatography and single-channel measurements for TM-gramicidin, and confirm the importance of indole hydrogen bonding for the conformation and function of ion channels and membrane proteins.

© 2013 Elsevier B.V. All rights reserved.

## 1. Introduction

Biological membranes represent complex two-dimensional, non-covalent assemblies of a diverse variety of lipids and proteins. They provide an identity to the cell and facilitate cellular communication and information processing. Membrane proteins are workhorses of the cellular machinery. About 30% of all proteins are predicted to be membrane proteins and ~50% of all proteins are membrane proteins for eukaryotic cells [1,2]. The crystallization efforts of membrane proteins in their native conditions are often complicated, and pose considerable challenge due to the intrinsic dependence of membrane

protein structure on surrounding membrane lipids [3]. Approaches based on NMR and fluorescence spectroscopy have proved useful in elucidating the organization, topology and orientation of membrane proteins and peptides [4,5]. An additional advantage of spectroscopic approaches is that the information obtained is dynamic in nature, necessary for understanding membrane protein function.

Transmembrane proteins and peptides have characteristic stretches of amino acids capable of interacting with the membrane bilayer and are reported to have a significantly higher tryptophan content than soluble proteins [6]. Tryptophan residues are believed to be crucial in the structure and function of membrane proteins and peptides [7–12]. A major observation is that tryptophans in membrane proteins and peptides are not uniformly distributed, but tend to be localized toward the membrane interface. Interestingly, the interfacial region in membranes is characterized by unique motional and dielectric properties, distinct from both the bulk aqueous phase and the hydrocarbon-like interior of the membrane [12,13]. A unique feature of tryptophan is its ability to participate in both hydrophobic and polar interactions. Among the naturally occurring amino acids, tryptophan shows the highest tendency to localize at the interface, based on partitioning of model peptides to membrane interfaces. Besides aromaticity and ring shape, hydrogen

**Abbreviations:** TM-gramicidin, tetramethyltryptophan gramicidin; POPC, 1-palmitoyl-2-oleoyl-sn-glycero-3-phosphocholine; DMPC, 1,2-dimyristoyl-sn-glycero-3-phosphocholine; DOPC, 1,2-dioleoyl-sn-glycero-3-phosphocholine; 5-PC, 1-palmitoyl-2-(5-doxyl)stearoyl-sn-glycero-3-phosphocholine; 12-PC, 1-palmitoyl-2-(12-doxyl)stearoyl-sn-glycero-3-phosphocholine; 2-AS, 2-(9-anthroyloxy)stearic acid; 12-AS, 12-(9-anthroyloxy)stearic acid; REES, red edge excitation shift; SUV, small unilamellar vesicles; CD, circular dichroism; LED, light emitting diode

\* Corresponding author. Tel.: +91 40 2719 2578; fax: +91 40 2716 0311.

E-mail address: [amit@ccmb.res.in](mailto:amit@ccmb.res.in) (A. Chattopadhyay).

<sup>1</sup> Present address: Room 10D14, 10 Center Drive, National Institute of Child Health and Human Development, National Institutes of Health, Bethesda, MD, USA.

bonding could play a role in the partitioning of the indole ring [8,14,15]. The overall role of tryptophan residues in the structure and function of membrane proteins and peptides is apparent from the observation that substitution or deletion of tryptophans often results in reduction or loss of their function [16–20].

The linear peptide gramicidin forms prototypical ion channels specific for monovalent cations and has been extensively used to explore the organization, dynamics, and function of membrane-spanning channels [21,22]. Gramicidin is a multi-tryptophan peptide (Trp-9, 11, 13, and 15; see Fig. 1a) which serves as an excellent model for transmembrane channels due to a number of reasons such as small size, ready availability and the relative ease with which chemical modifications can be performed. These special features make gramicidin unique among small membrane-active peptides and provide the basis for its use to explore the principles that govern the folding and function of membrane-spanning channels [21–23]. Interestingly, gramicidin channels share vital structural features involving ion selectivity with complex ion

channels such as KcsA potassium channels [24]. Gramicidin assumes a wide range of environment-dependent conformations due to its unique sequence of alternating L- and D-chirality. Two major conformations adopted by gramicidin in various environments are: (i) the single stranded  $\beta^{6,3}$  helical dimer (the 'channel' form), and (ii) the double stranded intertwined helix (collectively known as the 'nonchannel' form) [22]. The amino terminal-to-amino terminal single-stranded  $\beta^{6,3}$  helical dimer form is the thermodynamically preferred conformation in membranes and membrane-mimetic media. In this conformation, the tryptophan residues remain clustered at the membrane-water interface [25–28]. Interestingly, the membrane interfacial localization of tryptophan residues is absent in 'nonchannel' conformations and the tryptophan residues are distributed along the membrane axis [10,22,25]. Nonchannel conformations have been shown to exist in membranes with polyunsaturated lipids [29], and in membranes with increased acyl chain lengths under hydrophobic mismatch conditions [30,31].

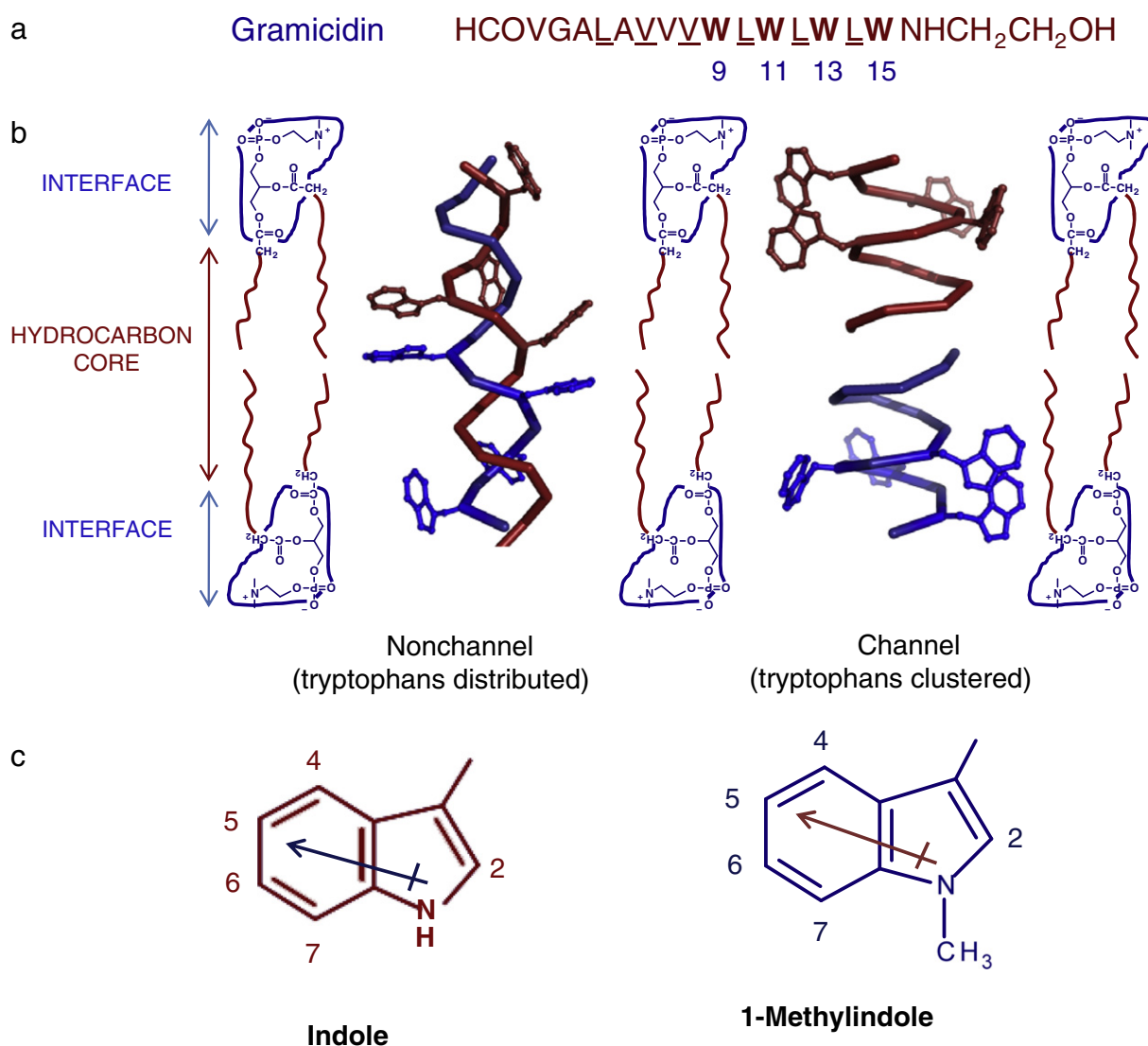


**Fig. 1.** (a) Amino acid sequence of gramicidin A highlighting the positions of the four tryptophans. Alternating D-amino acid residues are underlined. In the analog (TM-gramicidin) used in this study, four tryptophan residues in gramicidin are replaced by 1-methyltryptophan residues. (b) A schematic representation of the nonchannel and channel conformations of gramicidin showing the localization of tryptophan residues in the membrane bilayer. Tryptophans are clustered toward the membrane interface in the channel conformation. In contrast, tryptophans are distributed along the bilayer normal in the nonchannel conformation. See text for other details. Adapted and modified from Ref. [12]. (c) Chemical structures of indole and 1-methylindole. The major difference between indole and 1-methylindole is in their ability to form hydrogen bonds. While indole can form hydrogen bond with its –NH group, this ability is lost in 1-methylindole. Interestingly, the dipole moments of indole and 1-methylindole (shown as a vector) are similar in direction and magnitude. See text for other details. Adapted and modified from Ref. [43].

Gramicidin has proved to be a powerful model for elucidating the role of tryptophan at the membrane–water interface for maintaining ion channel structure and assembly [16,17,32–37]. The tryptophan residues in gramicidin channels have previously been shown to be crucial for the structure and function of the ion channel [16,17,32–35]. The importance of tryptophans is apparent from previous observations that the cation conductivity of the channel is reduced upon substitution of one or all of the tryptophan residues by phenylalanine, tyrosine or naphthylalanine [16,17,32], and also upon ultraviolet irradiation or chemical modification of the tryptophans [35,38,39]. It has been previously shown that gramicidins with Trp → Phe or Tyr substitutions have greater difficulty in forming membrane-spanning dimeric channels [16,35]. Unfortunately, these results do not provide information on the specific properties of tryptophan that contribute to the loss of channel structure and function. The loss in structure and function upon substitution of tryptophan with phenylalanine or tyrosine could be attributed to the loss of dipole moment, lack of hydrogen bonding ability, change in hydrophobicity, or a combination of these factors. Among these, the role of indole ring dipole moment was previously explored by using 5-fluorotryptophan instead of tryptophan [34,40]. This substitution increases the indole dipole moment without altering other properties.

In the context of the importance of hydrogen bonding in membrane protein structure and function [41,42], tryptophan residues were previously modified to 1-methyltryptophan in order to evaluate the contribution of the hydrogen bonding ability of tryptophans in maintaining the channel conformation of gramicidin (see Fig. 1c for the chemical structures of indole and 1-methylindole) [43]. Such modification results in the loss of hydrogen bonding ability of tryptophans. Yet, properties such as aromaticity and ring shape remain invariant. Importantly, the magnitude (~2.1 D for tryptophan and 2.2 D for 1-methyltryptophan) and direction of the dipole moment are not altered (see Fig. 1b) [43]. In this work, we explored the membrane organization and dynamics of the N-methylated tryptophan analog of gramicidin, i.e., tetramethyltryptophan gramicidin (TM-gramicidin), in which all four tryptophans are replaced by 1-methyltryptophan residues. We applied a combination of fluorescence approaches which include red edge excitation shift (REES) analysis, fluorescence lifetime and anisotropy measurements, membrane penetration depth measurement, and circular dichroism (CD) spectroscopy toward this goal. Our results show that in the absence of the hydrogen bonding ability of tryptophans, TM-gramicidin is not able to maintain the single stranded, head-to-head dimeric channel conformation in membranes. These results are consistent with recent single-channel and solid-state NMR results using TM-gramicidin [43].

## 2. Materials and methods

### 2.1. Materials

POPC, DOPC, 5-PC and 12-PC were obtained from Avanti Polar Lipids (Alabaster, AL). 2-AS and 12-AS were from Molecular Probes (Eugene, OR). Gramicidin A' (from *Bacillus brevis*) and DMPC were purchased from Sigma Chemical Co. (St. Louis, MO). TM-gramicidin was synthesized as described earlier [43]. Concentrations of both peptides were calculated using a molar extinction coefficient ( $\epsilon$ ) of  $20,700 \text{ M}^{-1} \text{ cm}^{-1}$  at 280 nm. Lipids were checked for purity by thin layer chromatography on silica gel precoated plates (Sigma) in chloroform/methanol/water (65:35:5, v/v/v) and were found to give a single spot in all cases when visualized upon charring with a solution containing cupric sulfate (10%, w/v) and phosphoric acid (8%, v/v) at  $150^\circ \text{C}$  [44]. The concentration of phospholipids was determined by phosphate assay subsequent to total digestion by perchloric acid [45]. DMPC was used as an internal standard to assess lipid digestion. All other chemicals used were of the highest purity available. Solvents used were of spectroscopic grade. Water was purified through a Millipore (Bedford, MA) Milli-Q system and used for all experiments.

### 2.2. Methods

#### 2.2.1. Sample preparation

Experiments were performed using SUV of POPC containing 2% (mol/mol) gramicidin or TM-gramicidin. In general, 1280 nmol of POPC in methanol was mixed with 25.6 nmol of gramicidin or TM-gramicidin in methanol. A few drops of chloroform were added to this solution. The solution was mixed well and dried under a stream of nitrogen while warming gently ( $\sim 40^\circ \text{C}$ ), and dried further under a high vacuum for at least 3 h. The dried film was swelled in 1.5 ml of 10 mM sodium phosphate, 150 mM sodium chloride, pH 7.2 buffer, and samples were vortexed for 3 min to uniformly disperse the lipid and peptide. Samples were sonicated to clarity under argon ( $\sim 50$  min in short bursts while being cooled in an ice/water mixture) using a Branson model 250 sonifier (Branson Ultrasonics, Danbury, CT) fitted with a microtip. The sonicated samples were centrifuged at 15,000 rpm in a Heraeus Biofuge centrifuge (DJB Labcare, Buckinghamshire, U.K.) for 15 min to remove the titanium particles shed from the microtip during sonication, and incubated for 12 h at  $65^\circ \text{C}$  with continuous shaking to convert to the channel conformation [46,47]. Samples were incubated in a dark at room temperature ( $\sim 25^\circ \text{C}$ ) for 1 h before fluorescence or CD measurements. Background samples were prepared the same way except that the peptide was omitted. All experiments were done with multiple sets of samples at room temperature ( $\sim 25^\circ \text{C}$ ).

#### 2.2.2. Circular dichroism (CD) measurements

CD measurements were carried out at room temperature ( $\sim 25^\circ \text{C}$ ) with a JASCO J-815 spectropolarimeter (Tokyo, Japan) calibrated with (+)-10-camphorsulfonic acid. Spectra were scanned in a quartz optical cell with a path length of 0.1 cm, and recorded in 0.5 nm wavelength increments and band width of 2 nm. For monitoring changes in secondary structure, spectra were scanned from 200 to 260 nm in the far-UV range. The scan rate was 50 nm/min and each spectrum is the average of 8 scans with a full scale sensitivity of 100 mdeg. Spectra were corrected for background by subtraction of appropriate blanks. Data are represented as mean residue ellipticities and calculated using the equation:

$$[\theta] = \theta_{\text{obs}} / (10Cl) \quad (1)$$

where  $\theta_{\text{obs}}$  is the observed ellipticity in mdeg,  $l$  is the path length in cm, and  $C$  is the concentration of peptide bonds in mol/l.

#### 2.2.3. Steady state fluorescence measurements

Steady state fluorescence measurements were performed with a Hitachi F-4010 spectrofluorometer (Tokyo, Japan) using 1 cm path length quartz cuvettes. Excitation and emission slits with a nominal bandpass of 5 nm were used for all measurements. Background intensities of samples in which the peptide was omitted were subtracted from each sample spectrum to cancel out any contribution due to the solvent Raman peak and other scattering artifacts. The spectral shifts obtained with different sets of samples were identical in most cases, or were within  $\pm 1$  nm of the ones reported. Fluorescence anisotropy measurements were performed at room temperature ( $\sim 25^\circ \text{C}$ ) using a Hitachi polarization accessory. Fluorescence anisotropy values were calculated from the equation [48]:

$$r = \frac{I_{\text{VV}} - G I_{\text{VH}}}{I_{\text{VV}} + 2G I_{\text{VH}}} \quad (2)$$

where  $I_{\text{VV}}$  and  $I_{\text{VH}}$  are the measured fluorescence intensities (after appropriate background subtraction) with the excitation polarizer vertically oriented and emission polarizer vertically and horizontally oriented, respectively.  $G$  is the grating correction factor and is the ratio of the efficiencies of the detection system for vertically and horizontally polarized lights, and is equal to  $I_{\text{HV}}/I_{\text{HH}}$ . All experiments were performed

with multiple sets of samples and average values of anisotropy are reported.

#### 2.2.4. Time-resolved fluorescence measurements

Fluorescence lifetimes were calculated from time-resolved fluorescence intensity decays using an IBH 5000F NanoLED equipment (Horiba Jobin Yvon, Edison, NJ) with DataStation software in the time-correlated single photon counting mode. A pulsed light emitting diode (LED) (NanoLED-17) was used as the excitation source. This LED generates optical pulse at 294 nm with a pulse duration less than 750 ps, and is run at a 1 MHz repetition rate. The LED profile (instrument response function) was measured at the excitation wavelength using Ludox (colloidal silica) as the scatterer. In order to optimize the signal to noise ratio, 10,000 photon counts were collected in the peak channel. All experiments were performed using emission slits with a bandpass of 6 nm or less. The sample and the scatterer were alternated after every 5% acquisition to ensure compensation for any shape and timing drifts that could occur during the period of data collection. This arrangement also prevents any prolonged exposure of the sample to the excitation beam, thereby avoiding any possible photodamage to the fluorophore. Data were stored and analyzed using DAS 6.2 software (Horiba Jobin Yvon, Edison, NJ). Fluorescence intensity decay curves so obtained were deconvoluted with the instrument response function and analyzed as a sum of exponential terms:

$$F(t) = \sum_i \alpha_i \exp(-t/\tau_i) \quad (3)$$

where  $F(t)$  is the fluorescence intensity at time  $t$  and  $\alpha_i$  is a pre-exponential factor representing the fractional contribution to the time-resolved decay of the component with a lifetime  $\tau_i$  such that  $\sum_i \alpha_i = 1$ . Decay parameters were recovered using a nonlinear least squares iterative fitting procedure based on the Marquardt algorithm [49]. The program also includes statistical and plotting subroutine packages [50]. The goodness of fit of a given set of observed data and the chosen function was evaluated by the  $\chi^2$  ratio, the weighted residuals [51], and the autocorrelation function of the weighted residuals [52]. A fit was considered acceptable when plots of the weighted residuals and the autocorrelation function showed random deviation about zero with a minimum  $\chi^2$  value not more than 1.4. Intensity-averaged mean lifetimes ( $\langle \tau \rangle$ ) for triexponential decays of fluorescence were calculated from the decay times and pre-exponential factors using the following equation [48]:

$$\langle \tau \rangle = \frac{\alpha_1 \tau_1^2 + \alpha_2 \tau_2^2 + \alpha_3 \tau_3^2}{\alpha_1 \tau_1 + \alpha_2 \tau_2 + \alpha_3 \tau_3} \quad (4)$$

#### 2.2.5. Depth measurements using the parallax method

The actual spin (nitroxide) content of the spin-labeled phospholipids (5- and 12-PC) was assayed using fluorescence quenching of anthroxyloxy-labeled fatty acids (2- and 12-AS) as described earlier [53]. For depth measurements, SUVs were prepared by sonication as described above (see Section 2.2.1). These samples were made with 160 nmol of DOPC containing a 15 mol% spin-labeled phospholipid (5- or 12-PC) and 3.2 nmol of TM-gramicidin. Duplicate samples were prepared in each case except for samples lacking the quencher (5- or 12-PC) where triplicates were prepared. Background samples lacking the peptide were prepared in all experiments, and their fluorescence intensities were subtracted from the respective sample fluorescence intensity.

### 3. Results

Circular dichroism spectroscopy is a convenient method to monitor conformations of gramicidin in membranes [25,36,43,54]. CD spectrum for the channel conformation of gramicidin displays two characteristic

peaks of positive ellipticity at ~218 and 235 nm, a valley at 230 nm, and a negative ellipticity below 208 nm. These are considered to be characteristic of the single-stranded  $\beta^{6.3}$  conformation. The nonchannel form of gramicidin exhibits a large negative peak at ~229 nm, a weaker positive peak at ~218 nm, and a positive ellipticity below 208 nm. We examined the backbone conformation of TM-gramicidin using CD spectroscopy in POPC in order to complement the CD spectra previously reported for the analog in DMPC and DOPC [43]. Fig. 2 shows the CD spectrum of TM-gramicidin. The figure also shows the spectrum for gramicidin in the channel conformation (induced by sonication followed by prolonged heat incubation at 65 °C) as a reference. Interestingly, the CD spectrum of TM-gramicidin resembles the spectral features of the nonchannel conformation.

The normalized fluorescence emission spectra of gramicidin and TM-gramicidin in POPC vesicles are shown in Fig. 3. The figure shows that tryptophans in the channel form of gramicidin display an emission maximum<sup>2</sup> of 333 nm (when excited at 280 nm) in agreement with previous results [25]. In contrast, the emission maximum of TM-gramicidin displays a significant red shift and is at 340 nm. Interestingly, the fluorescence of 1-methyltryptophan (the fluorophore in TM-gramicidin) has been reported to be sensitive to its immediate environment [55,56]. The relatively red-shifted emission maximum of TM-gramicidin could be indicative of the average environment experienced by 1-methyltryptophans in TM-gramicidin. It should be noted here that the emission maxima of gramicidin and TM-gramicidin in methanol do not differ appreciably (data not shown). The difference in the emission maximum observed in a membrane-bound condition therefore can be attributed to the conformational differences adopted by gramicidin and TM-gramicidin. We have previously reported a red-shifted emission maximum in the case of the nonchannel conformation of gramicidin [25].

The inset in Fig. 3 shows the relative fluorescence intensities of gramicidin and TM-gramicidin at their respective emission maximum. TM-gramicidin exhibits an appreciable increase (~3.5 fold) in fluorescence intensity relative to gramicidin. This could be attributed to both the photophysical properties of 1-methyltryptophan and the apparent nonchannel conformation of TM-gramicidin in POPC membranes. The quantum yield of 1-methyltryptophan has been reported to be higher than that of tryptophan [56], which could lead to an increase in fluorescence intensity for TM-gramicidin. We have earlier shown that the conformational change of gramicidin in membranes from the nonchannel to channel form is accompanied by a reduction in fluorescence intensity [25]. In other words, the nonchannel conformation is characterized by an increased fluorescence, possibly due to the fact that there is a distribution of tryptophans along the bilayer normal in this conformation. The increase in fluorescence intensity in the case of TM-gramicidin could therefore be due to the relatively nonpolar environment in which the fluorophore 1-methyltryptophan of TM-gramicidin is localized, since a reduction in polarity is associated with enhancement of fluorescence [55]. Yet another reason could be the release of quenching in the nonchannel conformation due to absence of aromatic–aromatic (stacking) interaction between the fluorophores at positions 9 and 15 observed in the channel conformation [28,37].

REES is defined as the shift in the wavelength of the maximum fluorescence emission toward higher wavelengths, caused by a shift in the excitation wavelength toward the red edge of the absorption band. This effect assumes relevance for polar fluorophores in a motionally restricted environment where the dipolar relaxation time for the

<sup>2</sup> We have used the term maximum of fluorescence emission in a somewhat broader sense here. In every case, we have monitored the wavelength corresponding to the maximum fluorescence intensity, as well as the center of mass of the fluorescence emission, in the symmetric part of the spectrum. In most cases, both these methods yielded the same wavelength. In cases where minor discrepancies were found, the center of mass of emission has been reported as the fluorescence maximum.



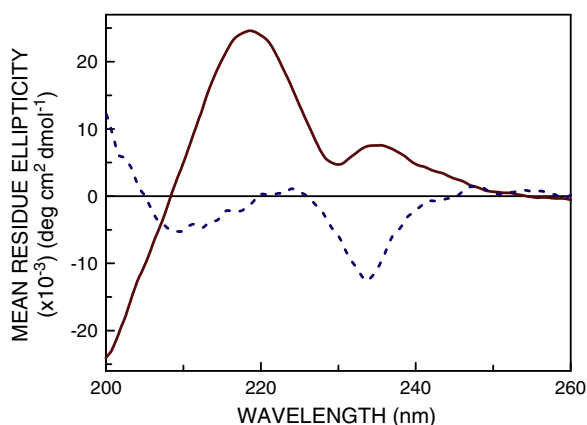


**Fig. 2.** Far-UV CD spectra of gramicidin (maroon, —), and TM-gramicidin (blue, - - -) in POPC vesicles. The ratio of peptide to POPC was 1:50 (mol/mol) and the concentration of POPC was 0.85 mM. See [Materials and methods](#) for other details.

solvent shell around a fluorophore becomes comparable to or longer than its fluorescence lifetime [12,13,57–60]. An attractive aspect of REES is that it allows the monitoring of the mobility parameters of the environment itself (represented by the relaxing solvent molecules) using the fluorophore merely as a reporter group. REES has proved to be a useful tool to monitor gramicidin conformations in membranes and membrane-mimetic environments [25,28,36,37,61,62].

**Fig. 4** shows the shifts in the maxima of fluorescence emission of gramicidin and TM-gramicidin as a function of excitation wavelength. The figure shows that the emission maximum of gramicidin is shifted from 333 to 340 nm in response to a change in excitation wavelength from 280 to 307 nm. This corresponds to a REES of 7 nm. TM-gramicidin, on the other hand, exhibits a relatively modest shift from 340 to 343 nm (corresponding to a REES of 3 nm), upon change in excitation wavelength from 280 to 307 nm. Such dependence of the emission maximum on excitation wavelength is representative of REES. It is possible that there could be further red shift upon excitation beyond 307 nm. We found it difficult to work in this wavelength range due to a low signal to noise ratio and artifacts due to the solvent Raman peak that sometimes remained even after background subtraction.

We previously reported that the magnitude of REES could be correlated with the vertical localization (depth) of the given fluorophore in the membrane [63]. Fluorophores present in the membrane interfacial region, characterized by restricted dynamics due to the mobility gradient

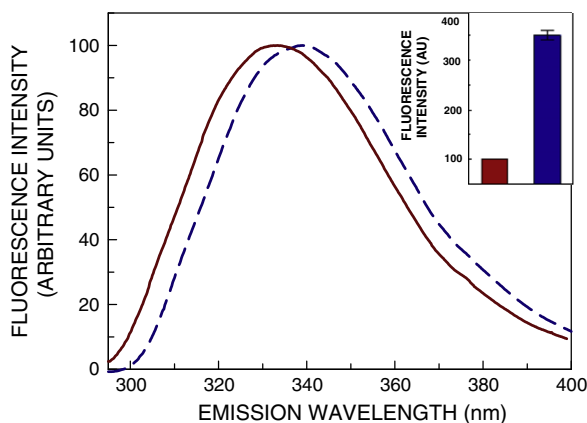


**Fig. 3.** Representative fluorescence emission spectra of gramicidin (maroon, —), and TM-gramicidin (blue, - - -) in POPC vesicles. The excitation wavelength was 280 nm in both cases. Spectra are intensity-normalized at the respective emission maximum. The inset shows relative fluorescence intensities of gramicidin and TM-gramicidin at their respective emission maximum. All other conditions are as in [Fig. 2](#). See [Materials and methods](#) for other details.

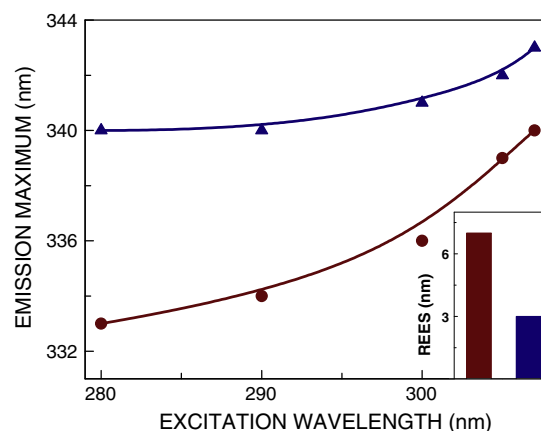


**Fig. 4.** Effect of changing excitation wavelength on the wavelength of maximum emission for gramicidin (maroon, ●), and TM-gramicidin (blue, ▲) in POPC vesicles. The lines joining data points are provided merely as viewing guides. The inset shows the magnitude of REES, which corresponds to the shift in emission maximum when the excitation wavelength was changed from 280 to 307 nm (color coding is the same). All other conditions are as in [Fig. 2](#). See [Materials and methods](#) for other details.

of membranes in the vertical (*z*) direction [64], display greater REES relative to fluorophores localized in the deeper (more fluid) regions of the membrane. The inset in **Fig. 4** shows that the magnitude of REES (3 nm) exhibited by TM-gramicidin is considerably less compared to REES (7 nm) of gramicidin in the channel conformation. As stated above, a characteristic feature of the tryptophan residues in the gramicidin channel conformation is that they remain clustered at the membrane–water interface [25–28]. However, this is not true for the nonchannel conformation where the tryptophan residues are distributed along the membrane axis [10,22,25]. As a result, the nonchannel conformation of gramicidin has earlier been characterized by modest REES [25]. The magnitude of REES exhibited by TM-gramicidin therefore indicates that the localization of fluorophores (1-methyltryptophan) in TM-gramicidin is deeper than the localization of tryptophans in gramicidin channels. This is also consistent with their lack of hydrogen bonding ability, since the membrane interface offers suitable chemistry for hydrogen bonding [13]. These results imply a nonchannel-like organization for TM-gramicidin in the membrane. This is in agreement with the results from CD measurements (see [Fig. 2](#)).

Fluorescence lifetime serves as a sensitive indicator of the local environment and polarity in which a given fluorophore is localized [65]. A typical decay profile of TM-gramicidin in POPC vesicles with its triexponential fitting and the statistical parameters used to check the goodness of fit are shown in [Fig. 5](#). The fluorescence lifetimes of gramicidin and TM-gramicidin are shown in [Table 1](#). Fluorescence decays could be fitted well with a triexponential function. The intensity-averaged mean fluorescence lifetimes (corresponding to emission at 340 nm) were calculated using Eq. (4) and are shown in [Fig. 6a](#). We chose to use the intensity-averaged mean fluorescence lifetime as an important parameter, since it is independent of the method of analysis and the number of exponentials used to fit the time-resolved fluorescence decay. [Fig. 6a](#) shows that the mean fluorescence lifetime of the tryptophan residues in gramicidin (~3.2 ns) is lower than that of 1-methyltryptophans in TM-gramicidin (~6.7 ns). The higher lifetime of TM-gramicidin could be due to the higher lifetime of 1-methyltryptophan compared to tryptophan [55,56]. The localization of the fluorophores in relatively nonpolar regions of the membrane in the nonchannel conformation of TM-gramicidin could also contribute to the higher lifetime since lifetimes tend to be shorter in polar environments due to faster deactivation processes [66].

The change in the mean fluorescence lifetime of gramicidin and TM-gramicidin as a function of increasing emission wavelength is shown in [Fig. 6b](#). The mean fluorescence lifetime exhibits a considerable increase in both cases with increasing emission wavelength from 330 to

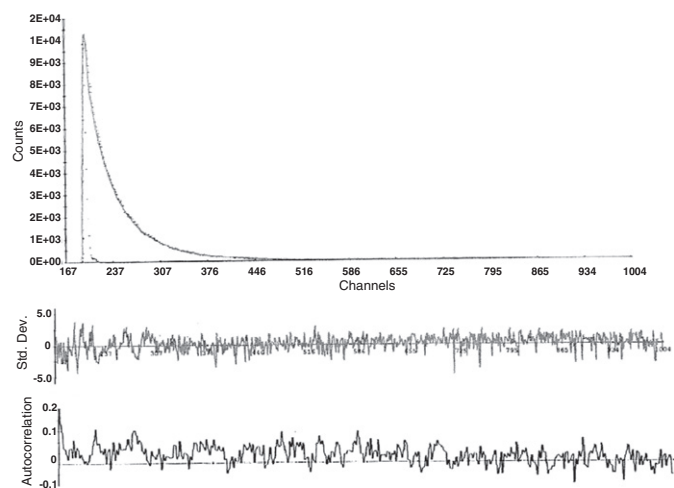


**Fig. 5.** Representative time-resolved fluorescence intensity decay of TM-gramicidin in POPC vesicles. Excitation wavelength was 294 nm corresponding to pulsed diode light source and emission was monitored at 330 nm. The sharp peak on the left corresponds to the profile of the pulsed light emitting diode (LED). The relatively broad peak on the right is the decay profile, fitted to a triexponential function. The two lower plots show the weighted residuals and the autocorrelation function of the weighted residuals. All other conditions are as in Fig. 2. See Materials and methods for other details.

370 nm. Similar observation of increasing lifetime with increasing emission wavelength has previously been reported for tryptophans in environments of restricted mobilities [28,67]. However, the extent of increase in mean fluorescence lifetime displayed considerable variation. The extent of increase in mean fluorescence lifetime with increasing wavelength was ~27% for gramicidin relative to ~11% in the case of TM-gramicidin. The difference in the extent of increase in fluorescence lifetime is indicative of the difference in their average microenvironment in the membrane. This is consistent with relatively large REES in gramicidin compared to TM-gramicidin (Fig. 4). Such increasing lifetimes across the emission spectrum may be interpreted in terms of solvent reorientation around the excited state fluorophore as follows [57]. Observation of emission spectra at shorter wavelengths selects for predominantly unrelaxed fluorophores. Their lifetimes are shorter since this sub-population is decaying both at the rate of fluorescence emission at the given excitation wavelength and by decay to longer (unobserved) wavelengths. On the other hand, observation at the longer emission wavelength (red edge) selects for the population of more relaxed fluorophores, which have spent enough time in the excited state to allow increasingly larger extents of solvent relaxation.

**Table 1**  
Representative fluorescence lifetimes of gramicidin and TM-gramicidin in POPC vesicles with increasing emission wavelength<sup>a</sup>

Emission wavelength (nm)	$\alpha_1$	$\tau_1$ (ns)	$\alpha_2$	$\tau_2$ (ns)	$\alpha_3$	$\tau_3$ (ns)
<i>(a) Gramicidin</i>						
330	0.16	0.15	0.63	1.48	0.21	4.32
340	0.12	0.22	0.65	1.61	0.23	4.86
350	0.13	0.12	0.61	1.58	0.26	4.80
360	0.11	0.12	0.61	1.62	0.28	5.07
370	0.13	0.11	0.56	1.65	0.31	5.12
<i>(b) TM-gramicidin</i>						
330	0.08	0.28	0.37	3.22	0.55	7.41
340	0.07	0.60	0.50	4.12	0.43	8.34
350	0.06	1.47	0.58	5.23	0.36	8.92
360	0.03	0.91	0.47	4.46	0.50	8.27
370	0.05	1.68	0.66	5.45	0.29	9.23

<sup>a</sup> Excitation wavelength was 294 nm. The number of photons collected at the peak channel was 10,000. All other conditions are as in Fig. 2. See Materials and methods for other details.

The fluorescence anisotropy of gramicidin and TM-gramicidin is shown in Fig. 7a. The anisotropy of gramicidin (0.12) was found to be higher than that of TM-gramicidin (0.04). To ensure that the reported anisotropy values are not influenced by lifetime-induced artifacts, the apparent (average) rotational correlation times were calculated using Perrin's equation [48]:

$$\tau_c = \frac{\langle \tau \rangle r}{r_0 - r} \quad (5)$$

where  $r_0$  is the limiting anisotropy of 1-methylindole or indole,  $r$  is the steady state anisotropy, and  $\langle \tau \rangle$  is the mean fluorescence lifetime taken from Fig. 6b. The values of the apparent rotational correlation times, calculated this way using a value of  $r_0$  of 0.30 for indole and 0.15 for 1-methylindole [68], are shown in Fig. 7b. As is evident from the figure, the apparent rotational correlation time of gramicidin (~2.1 ns) is lower relative to that of TM-gramicidin (~2.7 ns). This is in contrast to the trend observed in fluorescence anisotropy (see Fig. 7a). This implies that the apparent rotational correlation time, and not fluorescence anisotropy, is a correct indicator of rotational mobility in this case, since the latter could be influenced by a change in fluorescence lifetime. Based on these results, it appears that the increased bulk (steric hindrance) and hydrophobicity associated with the methyl group probably restricts the side chain motion of 1-methylindole in TM-gramicidin. This is in agreement with similar observations made using NMR for membrane-bound TM-gramicidin [43].

Membrane penetration depth [69–71] is an important parameter in the study of membrane peptides [25] and proteins [72], since knowledge of the depth of a membrane embedded group helps define the conformation and topology of membrane-bound molecules. In addition, a number of membrane properties vary in a depth-dependent manner [64]. More importantly, the membrane penetration depths of tryptophans in gramicidin serve as a useful indicator of its conformation. This is because the location, depth, orientation, and distribution of the tryptophan residues of gramicidin vary considerably in the channel and nonchannel conformations [25,27,33,36,37]. The distribution of tryptophans along the membrane axis is more extensive and the overall (average) locations of tryptophans are deeper in the nonchannel conformation [25,73,74]. To gain a better insight on the conformation of TM-gramicidin in membranes, penetration depths of its fluorophores (1-methyltryptophans) were determined. The average depth of these residues was calculated by the parallax method [69] using the equation:

$$z_{CF} = L_{C1} + \left\{ \left[ (-1/\pi C) \ln(F_1/F_2) - L_{21}^2 \right] / 2 L_{21} \right\} \quad (6)$$

where  $z_{CF}$  = the distance of the fluorophore from the center of the bilayer,  $L_{C1}$  = the distance of the center of the bilayer from the shallow quencher (5-PC in this case),  $L_{21}$  = the difference in depth between the two quenchers (i.e., the vertical distance between the shallow and the deep quencher), and  $C$  = the two-dimensional quencher concentration in the plane of the membrane (molecules/Å<sup>2</sup>). Here  $F_1/F_2$  is the ratio of  $F_1/F_0$  and  $F_2/F_0$  in which  $F_1$  and  $F_2$  are fluorescence intensities in the presence of the shallow (5-PC) and deep (12-PC) quencher, respectively, both at the same quencher concentration  $C$ ;  $F_0$  is the fluorescence intensity in the absence of any quencher. All bilayer parameters used were the same as described previously [69].

The average depth of penetration of 1-methyltryptophan residues in TM-gramicidin is shown in Table 2. The average depths of penetration of tryptophans in gramicidin in the channel and nonchannel conformations are shown as controls in the table. These results show that 1-methyltryptophan residues in TM-gramicidin are localized at a deeper region in the membrane, as apparent from the average depth of ~8 Å from the center of the bilayer (see Fig. 8). In comparison, the average depths of tryptophans in the channel and nonchannel conformations of gramicidin were earlier found to be ~11 and 7 Å from the center of the membrane, respectively [25]. Although these are average depths, they

are useful since they represent the lower limit of depth of penetration. The similarity in penetration depth between TM-gramicidin and the nonchannel conformation of gramicidin suggests that TM-gramicidin could adopt a nonchannel conformation under these conditions. This is in agreement with our data obtained from CD measurements (Fig. 2), and the red-shifted fluorescence emission spectrum displayed by TM-gramicidin (see Fig. 3).

#### 4. Discussion

The importance of tryptophan residues in maintaining the structure and function of membrane proteins and peptides is a subject of considerable interest [7,10,11,58,75–77]. Interestingly, the reason for the non-uniform distribution of tryptophan residues in integral membrane proteins and peptides is believed to be due to their involvement in hydrogen bonding [43,78] with the lipid carbonyl groups or interfacial water molecules. As a consequence, substitution or deletion of tryptophans in membrane proteins often results in reduction or loss of protein function [16–20]. As stated above, gramicidin channels represent an excellent model for exploring the principles underlying membrane protein structure and function, especially with respect to tryptophan residues. The anchoring property of tryptophans in the gramicidin channel has inspired the design of synthetic helical peptides,

having tryptophans as a common flanking motif, for studying lipid–protein interactions in membranes [79].

Gramicidin channels represent an excellent model for exploring the physicochemical principles underlying membrane protein structure and function. It was earlier shown that TM-gramicidin adopts a predominantly double stranded conformation in DMPC and DOPC bilayers [43]. Keeping in view the fact that DMPC bilayers are relatively thin compared to biological membranes, it was important to investigate the organization and dynamics of TM-gramicidin in the thicker and physiologically representative POPC bilayer membranes. In this work, we monitored the conformation and dynamics of the N-methylated analog of gramicidin (TM-gramicidin) in which the hydrogen bonding ability of tryptophan residues is masked due to methylation, using a variety of fluorescence approaches and CD spectroscopy. As stated above, an advantage of using methylated tryptophans is that it allows specific focus on the hydrogen bonding ability of tryptophans without altering other factors (such as dipole moment). Our results show that fluorescent analogs of tryptophan such as 1-methyltryptophan could be utilized to monitor the effect of hydrogen bonding of tryptophans in membrane-bound peptides and proteins utilizing their fluorescence.

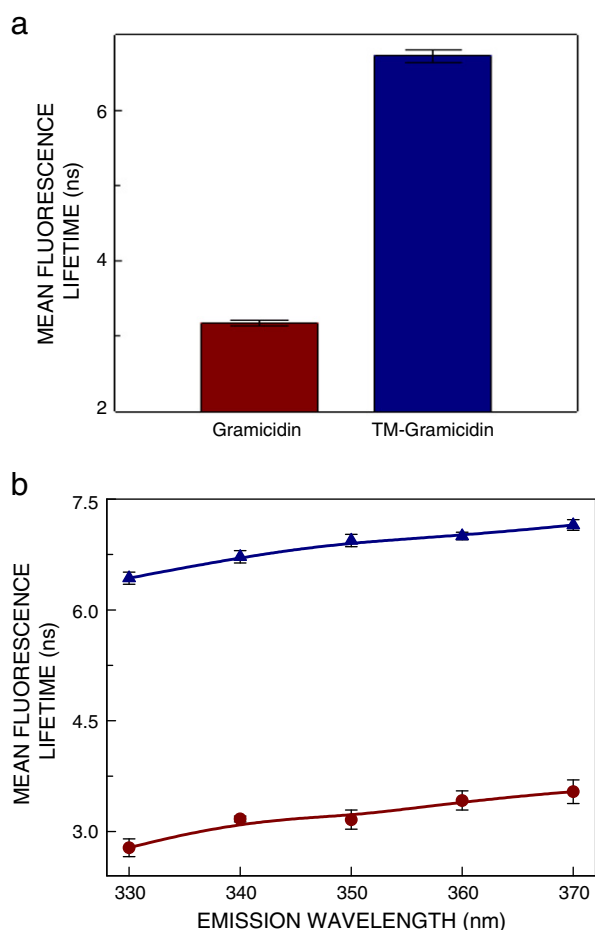


**Fig. 6.** (a) Mean fluorescence lifetime of gramicidin and TM-gramicidin in POPC vesicles. The excitation wavelength used was 294 nm and emission was fixed at 340 nm in both cases. (b) Mean fluorescence lifetime of gramicidin (maroon, ●) and TM-gramicidin (blue, ▲) in POPC vesicles with increasing emission wavelength. Mean fluorescence lifetimes were calculated from Table 1 using Eq. (4). Data shown are means  $\pm$  S.E. of three independent measurements. All other conditions are as in Fig. 2. See Materials and methods for other details.

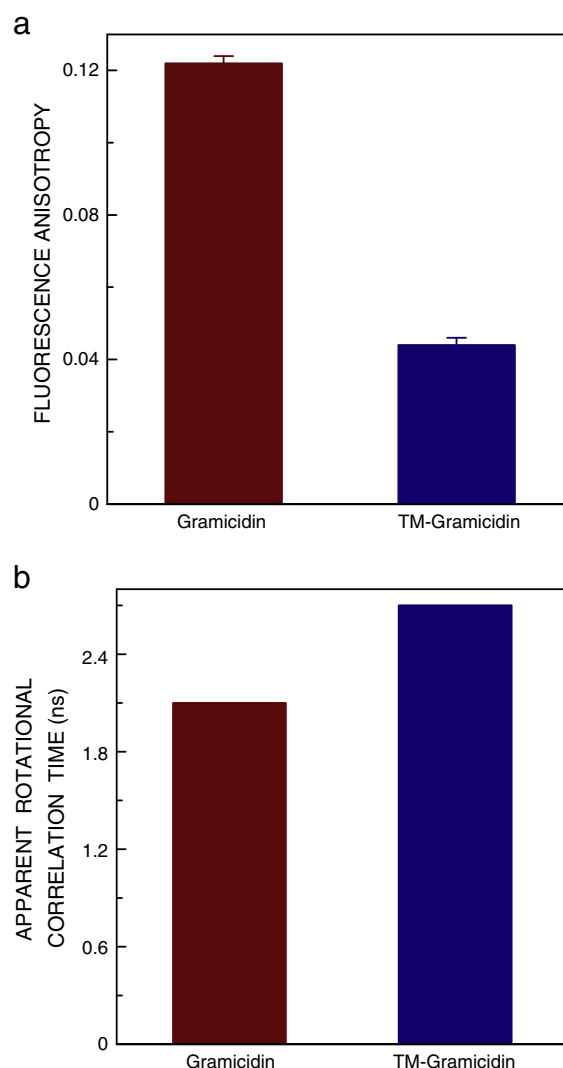


**Fig. 7.** (a) Fluorescence anisotropy and (b) apparent rotational correlation time of gramicidin and TM-gramicidin in POPC vesicles. The excitation wavelength was 295 nm and emission was monitored at 340 nm. Fluorescence anisotropy data shown are means  $\pm$  S.E. of at least three independent measurements. The apparent rotational correlation times were calculated using Eq. (5) (see text for other details). All other conditions are as in Fig. 2. See Materials and methods for other details.

**Table 2**  
Average membrane penetration depth by the parallax method<sup>a</sup>

Peptide	Distance from the center of the bilayer $z_{CF}$ (Å)
TM-gramicidin	8.1
Gramicidin (channel) <sup>b</sup>	11.0
Gramicidin (nonchannel) <sup>b</sup>	7.3

<sup>a</sup> Depths were calculated from fluorescence quencheds obtained with samples containing 15 mol% of 5-PC and 12-PC and using Eq. (6). Samples were excited at 280 nm, and emission was monitored at 335 nm. The ratio of peptide to total lipid was 1:50 (mol/mol). See [Materials and methods](#) for other details.

<sup>b</sup> From Ref. [25].

The carbonyl groups of ester lipids, lipid headgroups and water molecules present at membrane interface are all possible hydrogen bond acceptors. Previous work using Raman spectroscopy has indicated the formation of strong hydrogen bonds between lipid carbonyl groups and the indole –NH sites in the single stranded  $\beta^{6,3}$  gramicidin conformation in membranes [80]. In addition, molecular dynamics simulation of gramicidin in lipid bilayers has suggested that the interfacially localized tryptophan side chains form hydrogen bonds with ester carbonyl groups of lipids and membrane interfacial water molecules [81,82]. In addition, simulation studies with membrane proteins such as KcsA and OmpA have shown the existence of hydrogen bonds between tryptophan residues with interfacial water molecules and polar headgroups of lipids [83].

Our results show that TM-gramicidin is not able to maintain the single stranded, head-to-head dimeric channel conformation in membranes, thereby demonstrating the important role of indole hydrogen bonding in the channel conformation. These results, concerning the major gramicidin population, are in agreement with the previous results from size-exclusion chromatography, which demonstrated a conformational mixture of ~70% double stranded and only ~30% single stranded channel

conformation for TM-gramicidin [43]. Interestingly, when four phenylalanine residues are introduced into gramicidin instead of four tryptophan residues, the resulting tetraphenylalanine-gramicidin also lacks hydrogen bonding ability and folds <20% into the single stranded channel conformation [35]. As a consequence, we observe that TM-gramicidin exhibits a red-shifted fluorescence emission maximum, lower REES, and higher fluorescence intensity and lifetime (Figs. 3, 4 and 6a). These features of TM-gramicidin compare well with the nonchannel conformation of gramicidin [25]. The location (depth) of the 1-methyltryptophans in TM-gramicidin further enforces this conclusion. Unlike gramicidin channels, in which all the tryptophans are localized at the membrane interface, the average depth of 1-methyltryptophans in TM-gramicidin is more (see Table 2), a characteristic shared by the nonchannel form (as the majority population) [25]. The energy cost of burial of the indole in the hydrophobic core of the bilayer can provide the driving force for the conformational preference of gramicidin (single stranded channel or double stranded nonchannel). We conclude that coupled changes in the hydrogen bonding ability of tryptophan and peptide backbone structure are responsible for the loss of channel conformation. These results are consistent with previous size-exclusion, single-channel and solid-state NMR results using TM-gramicidin [43]. An additional message from our results is that fluorescence of 1-methyltryptophan could be effectively used as a tool to explore the hydrogen bonding ability of tryptophans in proteins and peptides.

We and others have previously shown that single tryptophan gramicidin analogs adopt predominantly nonchannel conformations [35,36]. In addition, we have recently shown that the positions of tryptophan residues in membranes are important for gramicidin structure and function [37,54]. We show here that the hydrogen bonding ability of tryptophans represents a crucial determinant in maintaining the gramicidin channel structure in the membrane. In a broader perspective, our results assume relevance in the context

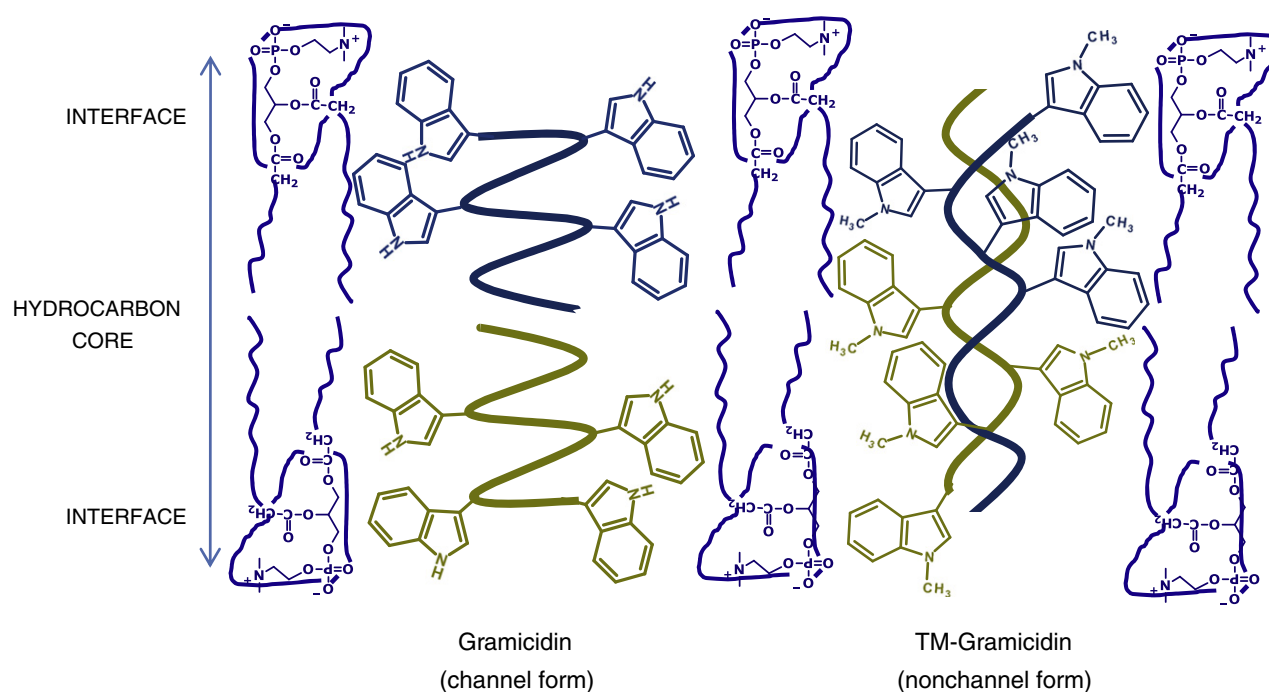


**Fig. 8.** Effect of 1-methyl substitution of tryptophan residues in the conformation of gramicidin. A schematic representation of the membrane bilayer showing the channel form of gramicidin and nonchannel form of TM-gramicidin. Our results suggest that the substitution of tryptophans with 1-methyltryptophan in gramicidin results in a conformation which is more nonchannel-like. The preferred locations of tryptophans (shown in olive and blue) in gramicidin channel are shown. It should be noted that tryptophan residues are preferentially localized in the membrane interface region in the channel form of gramicidin, whereas in the nonchannel conformation (as in the case of TM-gramicidin) the 1-methyltryptophan residues are distributed along the membrane axis. See Fig. 1 and text for details.



of the role of indole hydrogen bonding for the conformational and functional properties of ion channels and membrane proteins.

## Acknowledgements

This work was supported by the Council of Scientific and Industrial Research, Govt. of India (A.C.), and an NIH grant GM70971 to R.E.K. The peptide facility was supported by NIH grants GM103429 and GM103450, and by the Arkansas Biosciences Institute. S.H. and A.C. thank the Council of Scientific and Industrial Research for the award of Senior Research Fellowships. A.C. is an Adjunct Professor at the Special Centre for Molecular Medicine of Jawaharlal Nehru University (New Delhi, India) and Indian Institute of Science Education and Research (Mohali, India), and an Honorary Professor at the Jawaharlal Nehru Centre for Advanced Scientific Research (Bangalore, India). A.C. gratefully acknowledges the J.C. Bose Fellowship (Department of Science and Technology, Govt. of India). We thank the members of A.C.'s research group for critically reading the manuscript.

## References

- [1] E. Granseth, S. Seppälä, M. Rapp, D.O. Daley, G. von Heijne, Membrane protein structural biology – how far can the bugs take us, *Mol. Membr. Biol.* 24 (2007) 329–332.
- [2] L. Fagerberg, K. Jonasson, G. von Heijne, M. Uhlen, L. Berglund, Prediction of the human membrane proteome, *Proteomics* 10 (2010) 1141–1149.
- [3] L. Anson, Membrane protein biophysics, *Nature* 459 (2009) 343.
- [4] A. Chattopadhyay, H. Raghuraman, Application of fluorescence spectroscopy to membrane protein structure and dynamics, *Curr. Sci.* 87 (2004) 175–180.
- [5] M. Hong, Y. Zhang, F. Hu, Membrane protein structure and dynamics from NMR spectroscopy, *Annu. Rev. Phys. Chem.* 63 (2012) 1–24.
- [6] M. Schiffer, C.H. Chang, F.J. Stevens, The functions of tryptophan residues in membrane proteins, *Protein Eng.* 5 (1992) 213–214.
- [7] A. Chattopadhyay, S. Mukherjee, R. Rukmini, S.S. Rawat, S. Sudha, Ionization, partitioning, and dynamics of tryptophan octyl ester: implications for membrane-bound tryptophan residues, *Biophys. J.* 73 (1997) 839–849.
- [8] W.M. Yau, W.C. Wimley, K. Gawrisch, S.H. White, The preference of tryptophan for tryptophan analogs in ester- and ether-lipid bilayers studied by 2H NMR, *Biophys. J.* 75 (1998) 1365–1371.
- [9] J.A. Killian, G. von Heijne, How proteins adapt to a membrane–water interface, *Trends Biochem. Sci.* 25 (2000) 429–434.
- [10] D.A. Kelkar, A. Chattopadhyay, Membrane interfacial localization of aromatic amino acids and membrane protein function, *J. Biosci.* 31 (2006) 297–302.
- [11] R.E. Koeppe II, Concerning tryptophan and protein–bilayer interactions, *J. Gen. Physiol.* 130 (2007) 223–224.
- [12] S. Haldar, A. Chaudhuri, A. Chattopadhyay, Organization and dynamics of membrane probes and proteins utilizing the red edge excitation shift, *J. Phys. Chem. B* 115 (2011) 5693–5706.
- [13] A. Chattopadhyay, Exploring membrane organization and dynamics by the wavelength-selective fluorescence approach, *Chem. Phys. Lipids* 122 (2003) 3–17.
- [14] W.C. Wimley, S.H. White, Experimentally determined hydrophobicity scale for proteins at membrane interfaces, *Nat. Struct. Biol.* 3 (1996) 842–848.
- [15] S. Persson, J.A. Killian, G. Lindblom, Molecular ordering of interfacially localized tryptophan analogs in ester- and ether-lipid bilayers studied by 2H NMR, *Biophys. J.* 75 (1998) 1365–1371.
- [16] M.D. Becker, D.V. Greathouse, R.E. Koeppe II, O.S. Andersen, Amino acid sequence modulation of gramicidin channel function: effects of tryptophan-to-phenylalanine substitutions on the single-channel conductance and duration, *Biochemistry* 30 (1991) 8830–8839.
- [17] V. Fonseca, P. Daumas, L. Ranjalahy-Rasoloarijao, F. Heitz, R. Lazaro, Y. Trudelle, O.S. Andersen, Gramicidin channels that have no tryptophan residues, *Biochemistry* 31 (1992) 5340–5350.
- [18] A.S. Miller, J.J. Falke, Side chains at the membrane–water interface modulate the signaling state of a transmembrane receptor, *Biochemistry* 43 (2004) 1763–1770.
- [19] J.A. Lasalde, S. Tamamizu, D.H. Butler, C.R. Vibat, B. Hung, M.G. McNamee, Tryptophan substitutions at the lipid-exposed transmembrane segment M4 of *Torpedo californica* acetylcholine receptor govern channel gating, *Biochemistry* 35 (1996) 14139–14148.
- [20] S.Y. Wang, C. Russell, G.K. Wang, Tryptophan substitution of a putative D4S6 gating hinge alters slow inactivation in cardiac sodium channels, *Biophys. J.* 88 (2005) 3991–3999.
- [21] R.E. Koeppe II, O.S. Andersen, Engineering the gramicidin channel, *Annu. Rev. Biophys. Biomol. Struct.* 25 (1996) 231–258.
- [22] D.A. Kelkar, A. Chattopadhyay, The gramicidin ion channel: a model membrane protein, *Biochim. Biophys. Acta* 1768 (2007) 2011–2025.
- [23] O.S. Andersen, R.E. Koeppe II, Bilayer thickness and membrane protein function: an energetic perspective, *Annu. Rev. Biophys. Biomol. Struct.* 36 (2007) 107–130.
- [24] A. Chattopadhyay, D.A. Kelkar, Ion channels and D-amino acids, *J. Biosci.* 30 (2005) 147–149.
- [25] S.S. Rawat, D.A. Kelkar, A. Chattopadhyay, Monitoring gramicidin conformations in membranes: a fluorescence approach, *Biophys. J.* 87 (2004) 831–843.
- [26] A.M. O'Connell, R.E. Koeppe II, O.S. Andersen, Kinetics of gramicidin channel formation in lipid bilayers: transmembrane monomer association, *Science* 250 (1990) 1256–1259.
- [27] R.R. Ketchum, W. Hu, T.A. Cross, High-resolution conformation of gramicidin A in a lipid bilayer by solid-state NMR, *Science* 261 (1993) 1457–1460.
- [28] S. Mukherjee, A. Chattopadhyay, Motionally restricted tryptophan environments at the peptide–lipid interface of gramicidin channels, *Biochemistry* 33 (1994) 5089–5097.
- [29] S.V. Sychev, L.I. Barsukov, V.T. Ivanov, The double  $\pi\pi_5.6$  helix of gramicidin A predominates in unsaturated lipid membranes, *Eur. Biophys. J.* 22 (1993) 279–288.
- [30] M. Zein, R. Winter, Effect of temperature, pressure and lipid acyl chain length on the structure and phase behaviour of phospholipid–gramicidin bilayers, *Phys. Chem. Chem. Phys.* 2 (2000) 4545–4551.
- [31] D.A. Kelkar, A. Chattopadhyay, Modulation of gramicidin channel conformation and organization by hydrophobic mismatch in saturated phosphatidylcholine bilayers, *Biochim. Biophys. Acta* 1768 (2007) 1103–1113.
- [32] P. Daumas, F. Heitz, L. Ranjalahy-Rasoloarijao, R. Lazaro, Gramicidin A analogs: influence of the substitution of the tryptophans by naphthylalanines, *Biochimie* 71 (1989) 77–81.
- [33] W. Hu, K.-C. Lee, T.A. Cross, Tryptophans in membrane proteins: indole ring orientations and functional implications in the gramicidin channel, *Biochemistry* 32 (1993) 7035–7047.
- [34] O.S. Andersen, D.V. Greathouse, L.L. Providence, M.D. Becker, R.E. Koeppe II, Importance of tryptophan dipoles for protein function: 5-fluorination of tryptophans in gramicidin A channels, *J. Am. Chem. Soc.* 120 (1998) 5142–5146.
- [35] D. Salom, E. Pérez-Payá, J. Pascal, C. Abad, Environment- and sequence-dependent modulation of the double-stranded to single-stranded conformational transition of gramicidin A in membranes, *Biochemistry* 37 (1998) 14279–14291.
- [36] A. Chattopadhyay, S.S. Rawat, D.V. Greathouse, D.A. Kelkar, R.E. Koeppe II, Role of tryptophan residues in gramicidin channel organization and function, *Biophys. J.* 95 (2008) 166–175.
- [37] S. Haldar, A. Chaudhuri, H. Gu, R.E. Koeppe II, M. Kombrabail, G. Krishnamoorthy, A. Chattopadhyay, Membrane organization and dynamics of “inner pair” and “outer pair” tryptophan residues in gramicidin channels, *J. Phys. Chem. B* 116 (2012) 11056–11064.
- [38] C. Barth, G. Stark, Radiation inactivation of ion channels formed by gramicidin A. Protection by lipid double bonds and by  $\alpha$ -tocopherol, *Biochim. Biophys. Acta* 1066 (1991) 54–58.
- [39] A.A. Sobko, M.A. Vlasina, T.I. Rokitskaya, E.A. Kotova, S.D. Zakharov, W.A. Cramer, Y.N. Antonenko, Chemical and photochemical modification of colicin E1 and gramicidin A in bilayer lipid membranes, *J. Membr. Biol.* 199 (2004) 51–62.
- [40] D.D. Busath, C.D. Thulin, R.W. Hendershot, L.R. Phillips, P. Maughan, C.D. Cole, N.C. Bingham, S. Morrison, L.C. Baird, R.J. Hendershot, M. Cotten, T.A. Cross, Noncontact dipole effects on channel permeation. I. Experiments with (5F-indole)Trp<sup>13</sup> gramicidin A channels, *Biophys. J.* 75 (1998) 2830–2844.
- [41] S.H. White, How hydrogen bonds shape membrane protein structure, *Adv. Protein Chem.* 72 (2005) 157–172.
- [42] G. Grigoryan, W.F. Degrad, Modest membrane hydrogen bonds deliver rich results, *Nat. Chem. Biol.* 4 (2008) 393–394.
- [43] H. Sun, D.V. Greathouse, O.S. Andersen, R.E. Koeppe II, The preference of tryptophan for membrane interfaces: insights from N-methylation of tryptophans in gramicidin channels, *J. Biol. Chem.* 283 (2008) 22233–22243.
- [44] C.B. Baron, R.F. Coburn, Comparison of two copper reagents for detection of saturated and unsaturated neutral lipids by charring densitometry, *J. Liq. Chromatogr.* 7 (1984) 2793–2801.
- [45] C.W.F. McClure, An accurate and convenient organic phosphorus assay, *Anal. Biochem.* 39 (1971) 527–530.
- [46] J.A. Killian, K.U. Prasad, D. Hains, D.W. Urry, The membrane as an environment of minimal interconversion. A circular dichroism study on the solvent dependence of the conformational behavior of gramicidin in diacylphosphatidylcholine model membranes, *Biochemistry* 27 (1988) 4848–4855.
- [47] P.V. LoGrasso, F. Moll, T.A. Cross, Solvent history dependence of gramicidin A conformations in hydrated lipid bilayers, *Biophys. J.* 54 (1988) 259–267.
- [48] J.R. Lakowicz, Principles of Fluorescence Spectroscopy, 3rd ed. Springer, New York, 2006.
- [49] P.R. Bevington, Data Reduction and Error Analysis for the Physical Sciences, McGraw-Hill, New York, 1969.
- [50] D.V. O'Connor, D. Phillips, Time-correlated Single Photon Counting, Academic Press, London, 1984, 180–189.
- [51] R.A. Lampert, L.A. Chewter, D. Phillips, D.V. O'Connor, A.J. Roberts, S.R. Meech, Standards for nanosecond fluorescence decay time measurements, *Anal. Chem.* 55 (1983) 68–73.
- [52] A. Grinvald, I.Z. Steinberg, On the analysis of fluorescence decay kinetics by the method of least-squares, *Anal. Biochem.* 59 (1974) 583–598.
- [53] F.S. Abrams, E. London, Extension of the parallax analysis of membrane penetration depth to the polar region of model membranes: use of fluorescence quenching by a spin-label attached to the phospholipid polar headgroup, *Biochemistry* 32 (1993) 10826–10831.
- [54] H. Gu, K. Lum, J.H. Kim, D.V. Greathouse, O.S. Andersen, R.E. Koeppe II, The membrane interface dictates different anchor roles for “inner pair” and “outer pair” tryptophan indole rings in gramicidin A channels, *Biochemistry* 50 (2011) 4855–4866.
- [55] S.R. Meech, D. Phillips, A.G. Lee, On the nature of the fluorescent state of methylated indole derivatives, *Chem. Phys.* 80 (1983) 317–328.

- [56] M.R. Eftink, J. Jia, D. Hu, C.A. Ghiron, Fluorescence studies with tryptophan analogs: excited state interactions involving the side chain amino group, *J. Phys. Chem.* 99 (1995) 5713–5723.
- [57] S. Mukherjee, A. Chattopadhyay, Wavelength-selective fluorescence as a novel tool to study organization and dynamics in complex biological systems, *J. Fluoresc.* 5 (1995) 237–246.
- [58] H. Raghuraman, D.A. Kelkar, A. Chattopadhyay, Novel insights into protein structure and dynamics utilizing the red edge excitation shift approach, in: C.D. Geddes, J.R. Lakowicz (Eds.), *Reviews in Fluorescence* 2005, vol. 2, Springer, New York, 2005, pp. 199–224.
- [59] A.P. Demchenko, Site-selective red-edge effects, *Methods Enzymol.* 450 (2008) 59–78.
- [60] A. Chattopadhyay, S. Haldar, Dynamic insight into protein structure utilizing red edge excitation shift, *Acc. Chem. Res.* (2013) (in press).
- [61] D.A. Kelkar, A. Chattopadhyay, Effect of graded hydration on the dynamics of an ion channel peptide: a fluorescence approach, *Biophys. J.* 88 (2005) 1070–1080.
- [62] S.S. Rawat, D.A. Kelkar, A. Chattopadhyay, Effect of structural transition of the host assembly on dynamics of an ion channel peptide: a fluorescence approach, *Biophys. J.* 89 (2005) 3049–3058.
- [63] A. Chattopadhyay, S. Mukherjee, Depth-dependent solvent relaxation in membranes: wavelength-selective fluorescence as a membrane dipstick, *Langmuir* 15 (1999) 2142–2148.
- [64] S. Haldar, M. Kombrabail, G. Krishnamoorthy, A. Chattopadhyay, Depth-dependent heterogeneity in membranes by fluorescence lifetime distribution analysis, *J. Phys. Chem. Lett.* 3 (2012) 2676–2681.
- [65] F.G. Prendergast, Time-resolved fluorescence techniques: methods and applications in biology, *Curr. Opin. Struct. Biol.* 1 (1991) 1054–1059.
- [66] W.B. De Lauder, Ph. Wahl, Effect of solvent upon the fluorescence decay of indole, *Biochim. Biophys. Acta* 243 (1971) 153–163.
- [67] A.K. Ghosh, R. Rukmini, A. Chattopadhyay, Modulation of tryptophan environment in membrane-bound melittin by negatively charged phospholipids: implications in membrane organization and function, *Biochemistry* 36 (1997) 14291–14305.
- [68] M.R. Eftink, L.A. Selvidge, P.R. Callis, A.A. Rehms, Photophysics of indole derivatives: experimental resolution of  $L_a$  and  $L_b$  transitions and comparison with theory, *J. Phys. Chem.* 94 (1990) 3469–3479.
- [69] A. Chattopadhyay, E. London, Parallax method for direct measurement of membrane penetration depth utilizing fluorescence quenching by spin-labeled phospholipids, *Biochemistry* 26 (1987) 39–45.
- [70] A. Chattopadhyay, Membrane penetration depth analysis using fluorescence quenching: a critical review, in: B.P. Gaber, K.R.K. Easwaran (Eds.), *Biomembrane Structure and Function: the State of the Art*, Adenine Press, Schenectady, New York, 1992, pp. 153–163.
- [71] E. London, A.S. Ladokhin, Measuring the depth of amino acid residues in membrane-inserted peptides by fluorescence quenching, in: D. Benos, S. Simon (Eds.), *Current Topics in Membranes*, Elsevier, San Diego, CA, 2002, pp. 89–115.
- [72] A. Chattopadhyay, M.G. McNamee, Average membrane penetration depth of tryptophan residues of the nicotinic acetylcholine receptor by the parallax method, *Biochemistry* 30 (1991) 7159–7164.
- [73] S. Haldar, M. Kombrabail, G. Krishnamoorthy, A. Chattopadhyay, Monitoring membrane protein conformational heterogeneity by fluorescence lifetime distribution analysis using the maximum entropy method, *J. Fluoresc.* 20 (2010) 407–413.
- [74] S. Arumugam, S. Pascal, C.L. North, W. Hu, K.-C. Lee, M. Cotten, R.R. Ketchum, F. Xu, M. Brennen, F. Kovacs, F. Tian, A. Wang, S. Huo, T.A. Cross, Conformational trapping in a membrane environment: a regulatory mechanism for protein activity? *Proc. Natl. Acad. Sci. U. S. A.* 93 (1996) 5872–5876.
- [75] F.R. Svensson, P. Lincoln, B. Nordén, E.K. Esbjörner, Tryptophan orientations in membrane-bound gramicidin and melittin – a comparative linear dichroism study on transmembrane and surface-bound peptides, *Biochim. Biophys. Acta* 1808 (2011) 219–228.
- [76] E.F. Haney, A.P. Petersen, C.K. Lau, W. Jing, D.G. Storey, H.J. Vogel, Mechanism of action of puromycin derived tryptophan-rich antimicrobial peptides, *Biochim. Biophys. Acta* 1828 (2013) 1802–1813.
- [77] E.K. Esbjörner, C.E.B. Caesar, B. Albinsson, P. Lincoln, B. Nordén, Tryptophan orientation in model lipid membranes, *Biochem. Biophys. Res. Commun.* 361 (2007) 645–650.
- [78] J.A. Ippolito, R.S. Alexander, D.W. Christianson, Hydrogen bond stereochemistry in protein structure and function, *J. Mol. Biol.* 215 (1990) 457–471.
- [79] V.V. Vostrikov, A.E. Daily, D.V. Greathouse, R.E. Koeppe II, Charged or aromatic anchor residue dependence of transmembrane peptide tilt, *J. Biol. Chem.* 285 (2010) 31723–31730.
- [80] M. Bouchard, M. Auger, Solvent history dependence of gramicidin–lipid interactions: a Raman and infrared spectroscopic study, *Biophys. J.* 65 (1993) 2484–2492.
- [81] T.B. Woolf, B. Roux, Molecular dynamics simulation of the gramicidin channel in a phospholipid bilayer, *Proc. Natl. Acad. Sci. U. S. A.* 91 (1994) 11631–11635.
- [82] F.N.R. Petersen, M.Ø. Jensen, C.H. Nielsen, Interfacial tryptophan residues: a role for the cation– $\pi$  effect? *Biophys. J.* 89 (2005) 3985–3996.
- [83] C. Domene, P.J. Bond, S.S. Deol, M.S.P. Sansom, Lipid/protein interactions and the membrane/water interfacial region, *J. Am. Chem. Soc.* 125 (2003) 14966–14967.